Journal of Power Sources 180 (2008) 803–807

Contents lists available at ScienceDirect

Journal of Power Sources

journal homepage: www.elsevier.com/locate/jpowsour

Short communication

Austenitic stainless steels in high temperature phosphoric acid

Heli Wang*, John A. Turner

National Renewable Energy Laboratory, 1617 Cole Boulevard, Golden, CO 80401, USA

ARTICLE INFO

Article history:
Received 1 February 2008
Received in revised form 20 February 2008
Accepted 21 February 2008
Available online 18 March 2008

Keywords:
Stainless steel
Phosphoric acid
XPS
Bipolar plate
High temperature

ABSTRACT

Austenite 316 L, 317 L, and 904 L stainless steels were investigated in 98% H_3PO_4 at 170 °C and they experienced passivation regardless of the purged gas. When polarized at 0.1 V (hydrogen) and 0.7 V (air) (phosphoric acid fuel cell (PAFC) environments), currents at the level of mA cm^{-2} were observed. Compared to carbon composite under identical conditions, 904 L showed lower currents while 316 L and 317 L showed much higher currents.

X-ray photoelectron spectroscopy (XPS) depth profiles indicated that the surface film of the fresh steels consists of a Fe-oxide-rich outer layer and a Cr-oxide-rich inner layer. After being polarized in the PAFC environments, the Fe-oxide layer was selectively dissolved and Cr-oxide dominated the passive film. Phosphorus was incorporated into the film during the process, thus the chemical composition of the passive film differed from those formed in the polymer electrolyte membrane fuel cell (PEMFC) environments. The thicknesses of the stainless steels in the passive films in PAFC environments were estimated.

1. Introduction

The polymer electrolyte membrane fuel cell (PEMFC) is a highly efficient chemical energy converter. However, many technical and economic barriers still prevent it from a broad application in the civilian market. Among the barriers are the high cost of the traditional machined graphite bipolar plates and the degradation of the catalyst by trace CO in the fuel [1]. Moreover, the transportation industry prefers an operating temperature near 120 °C so that most of the existing heat management sub-system in a vehicle can be reused and will not need to be redesigned. Additionally, if the PEMFC can be operated at temperatures above 120 °C, better utilization of the generated heat is possible. This would lead to a higher efficiency compared with operation at 70–90 °C. The poisoning effect of trace CO on the catalyst could also be significantly reduced at this temperature. Operation at higher temperatures has advantages and is a focus point in the DOE fuel cell program [2].

Among the issues seldom discussed in the application of high temperature membranes for fuel cells are the material requirements for bipolar plates. Classic machined graphite is clearly not viable for mass production and the alternatives have not been studied in detail. Research on the PEMFC bipolar plates at high temperatures has many challenges. At normal atmospheric pressure, an aqueous solution is not available at temperatures over 100 °C. Phosphoric acid is a good candidate electrolyte for high temperature bipolar plate studies due to its application in the phosphoric acid fuel cell (PAFC). Above 150 °C, H_3PO_4 is predominantly in the polymeric state and is strongly ionized with reasonably good electrolyte conductivity. The PAFC can tolerate 1–2% CO in this temperature range [3]. Other advantages of the H_3PO_4 electrolyte include its stability in the electrochemical environment up to at least 225 °C and a low vapor pressure [3]. Stainless steels have been shown to have favorable properties as bipolar plates for current PEMFC technology [4–18]; however, we have not seen any studies on their application in a phosphoric acid environment. In this paper we will focus on the corrosion behavior of austenite stainless steels in phosphoric acid electrolyte at 170 °C, the actual PAFC operating temperature.

2. Experimental

2.1. Materials and electrodes

Stainless steel plates of 316 L and 317 L were provided by J&L Specialty Steel, Inc. (now part of Allegheny Ludlum Corp.), while 904 L (Fe–20Cr–25Ni–4.5Mo–1.5Mn–1Cu) was purchased from Metalmen Sales, Inc. The chemical compositions are described elsewhere [16]. The plates were cut into samples of 2.5 cm × 1.3 cm, polished with #600 grit SiC paper, rinsed with acetone, and dried with pressured nitrogen gas.

For electrode preparation, one side of the sample was connected to a copper wire with silver paint. After drying, the side with the electrical contact and the edges of the sample were covered with a high temperature epoxy. It should be mentioned that phosphoric acid at 170 °C is very aggressive towards epoxy and our standard

* Corresponding author. Tel.: +1 303 275 3858; fax: +1 303 275 2905.
E-mail address: heli_wang@nrel.gov (H. Wang).

0378-7753/$ – see front matter © 2008 Elsevier B.V. All rights reserved.
doi:10.1016/j.jpowsour.2008.02.086

epoxies failed in this environment. Considerable effort was focused on identifying suitable epoxies for sealing the samples. Over 12 different high temperature sealants were tested and we determined that one of them (Duralco 4700, Cotronics Corp.) could work for 3–5 h in the environment when the epoxy was cured 4 h at 120 °C and then 1 h at 165 °C. We also found it advantageous to repeat the epoxy coat; thus repeating the sealing process to eliminate leakage.

2.2. Electrochemistry

Reagent grade 98% H_3PO_4 was purchased from Sigma–Aldrich, Inc. H_3PO_4 is a solid crystal at room temperature, but will melt at temperatures over *ca.* 40 °C. The electrochemical tests were carried out at 170 °C; the temperature was controlled by means of a circulating bath.

Some additional modifications of the test system were necessary for operating in the 100–200 °C range suitable for the phosphoric acid electrolyte. We identified the proper tubing material for the high temperature control bath. The electrochemical measurements used a conventional three-electrode system, in which a platinum sheet acted as the counter electrode and a 0.5 mm diameter palladium wire with purity better than 99.9% (Sigma–Aldrich, Inc.) acted as the reference electrode. It is generally accepted that this type of reference electrode provides a reasonable approximation of the reversible hydrogen electrode (RHE) when immersed directly into the electrolyte. Therefore, all potentials will be referred to RHE except as otherwise noted. We used a Solartron 1287 potentiostat interfaced with a PC to conduct the tests. Depending on the environment to be simulated, hydrogen gas or pressured air was used to purge the electrolyte prior to and during the tests. For dynamic polarization, samples were stabilized at the open circuit potential (OCP) for 5 min then a potential scan towards the anodic direction was started from the OCP, at a scanning rate of 1 mV s^{-1}. Potentiostatic polarization was used to investigate the anodic behavior of the alloys in the simulated PAFC environments. Based on the PAFC industry practice, two potentials were selected for the tests: 0.1 V for the anode environment and 0.7 V for the cathode environment. In the former case, the electrolyte was purged with hydrogen gas, and in the later case pressured air was used to purge the electrolyte.

2.3. Surface characterization with X-ray photoelectron spectroscopy (XPS)

To identify the influence of polarization on passive film formation, the surfaces of fresh and polarized samples were investigated by means of XPS. The procedure for the XPS experiments has been described previously [17,18]. In short, they were carried out in a Phi 5600 electron spectrometer using an Al Kα radiation X-ray source (1486.6 eV) and a hemispherical energy analyzer. The base pressure in the spectrometer chamber was 1.33×10^{-8} Pa. The depth profiles were obtained by sputtering with 3 keV argon ions. During the sputtering process, the argon pressure in the chamber was 6.67×10^{-5} Pa. The sputtering rate, based on a calibration by sputtering off a thin film, was 14 Å min^{-1}.

3. Results and discussion

3.1. Dynamic polarization

When the potential is scanned towards more positive potentials, stainless steels experience passivation under both air and hydrogen conditions. Typical dynamic polarization curves for 316 L stainless steel in 98% H_3PO_4 at 170 °C, purged either with hydrogen gas or pressured air, are shown in Fig. 1. The OCPs for 316 L are *ca.* −0.33 V in air-purged electrolyte and *ca.* −0.21 V in H_2-purged electrolyte.

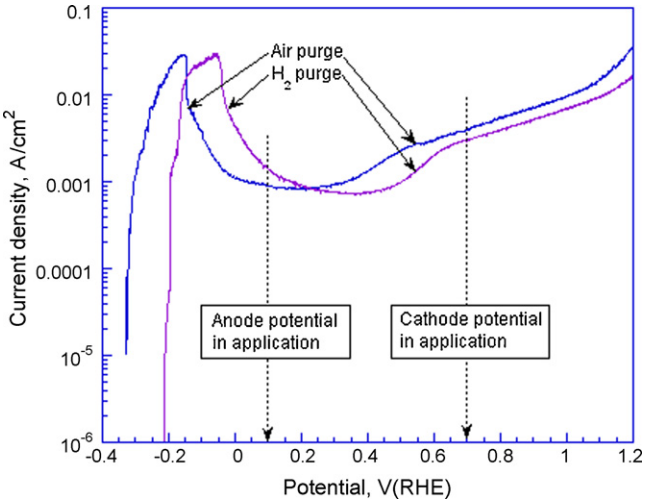

Fig. 1. Dynamic polarization of 316 L stainless steel in H_3PO_4 at 170 °C purged either with hydrogen gas or air. Application potentials in typical phosphoric acid fuel cell (PAFC) are marked in the plot.

The OCPs for 317 L are *ca.* −0.34 V in air-purged electrolyte and *ca.* −0.25 V in H_2-purged electrolyte; those for 904 L are *ca.* −0.25 V in air-purged electrolyte and *ca.* −0.20 V under H_2-purge. Passivation occurs at *ca.* −0.15 V in air-purge and at *ca.* −0.06 V in H_2-purged electrolyte for 316 L; at *ca.* −0.17 V in air-purge and at *ca.* −0.13 V in H_2-purge for 317 L; and at *ca.* −0.19 V in air-purge and at *ca.* −0.12 V in the H_2-purge for 904 L. Passivating currents (the current at the peak) are *ca.* 29–30 mA cm^{-2} for 316 L regardless of the purge gases; *ca.* 32 mA cm^{-2} in air-purged conditions and *ca.* 17 mA cm^{-2} in hydrogen conditions for 317 L; and *ca.* 4.7 mA cm^{-2} in air-purged electrolyte and *ca.* 6.6 mA cm^{-2} in H_2-purged electrolyte for 904 L. A lower passivating current for 904 L than the rest suggests that this alloy has a better corrosion resistance in this environment.

Under air-purge conditions, 316 L is passivated until *ca.* 0.50 V, followed by a Tafel region to *ca.* 1.10 V then trans-passivation occurs. The polarization curve under H_2-purge is shifted, with a Tafel region at *ca.* 0.63–1.15 V. Similar polarization curves are obtained with 317 L, where Tafel regions are at *ca.* 0.68–1.05 V in air-purged electrolyte and at *ca.* 0.85–1.15 V in the H_2-purged electrolyte. 904 L has a wider passivation region. For 904 L in the electrolyte purged with air, some secondary current peaks are observed at *ca.* 0.60 V and *ca.* 0.85 V (not shown), but are not seen in the H_2-purged electrolyte. The explanation for these peaks is likely related to the oxidation of the Cr_2O_3 in the passive film to a higher valence state. A similar peak was observed for high Cr-bearing AISI446 steel in the PEMFC environment [17]. Transpassivation occurs at *ca.* 0.95 V in air-purged electrolyte and at *ca.* 1.05 V in H_2-purged electrolyte with 904 L steel.

3.2. Potentiostatic polarization

Fig. 2 shows the potentiostatic polarizations for the stainless steels at 0.1 V in H_3PO_4 and 170 °C purged with hydrogen gas (PAFC anode environment). All steels experienced a sharp current drop as soon as the potential was applied, followed by a current recovery. The recovery took *ca.* 5 min for 316 L, *ca.* 6.5 min for 317 L, and *ca.* 15 min for 904 L, inset of Fig. 2. After this recovery, the current was reasonably stable although there was a slow current increase. It reached *ca.* 2.85 mA cm^{-2} for 316 L, *ca.* 2.35 mA cm^{-2} for 317 L, and *ca.* 1.43 mA cm^{-2} for 904 L by the end of the test.

Fig. 3 gives the potentiostatic polarizations at 0.7 V for the stainless steels in H_3PO_4 at 170 °C purged with air (PAFC cathode

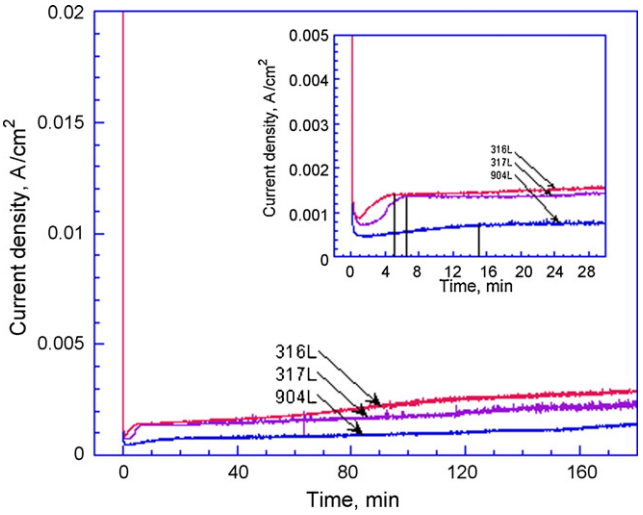

Fig. 2. Potentiostatic polarization of stainless steels at 0.1 V in H_3PO_4 at 170 °C purged with hydrogen gas. Inset shows the current decay during the first 30 min polarization.

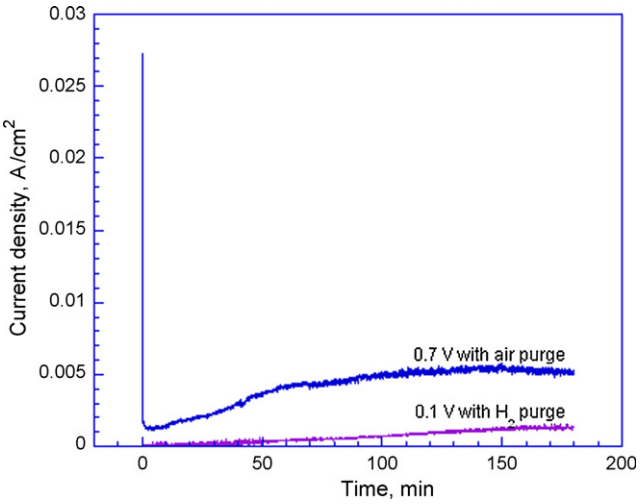

Fig. 4. Anodic behavior of carbon composite in 98% H_3PO_4 at 170 °C. Applied potentials and purged gases are marked in the plot.

environment). Again, all steels experienced a sharp current drop as soon as the potential was applied, followed by a secondary current peak. From the inset of Fig. 3, the secondary peaks are located at 1 min for 316 L, 2 min for 317 L, and 5 min for 904 L. After the peak, the current stabilizes. These peaks seem to be related to the current stabilization in Fig. 2. Three hundred and sixteen liter keeps a reasonably stable current at 5.0–5.8 mA cm^{-2} for the whole test period; the current for 317 L shows some increase after recovery and reaches *ca.* 5.0 mA cm^{-2} at the end of the test. The current for 904 L is much lower than the rest, reaching *ca.* 1.7 mA cm^{-2} by the end of the test, although it stays around 1.0–1.2 mA cm^{-2} during most of the test period. Such current levels are higher than the μA cm^{-2} level for the stainless steels in 1 M H_2SO_4 solution of 70 °C with the same purged gases.

For comparison, the behavior of carbon composite bipolar plate samples obtained from PlugPower was studied in identical conditions. Potentiostatic polarizations in PAFC environments (Fig. 4) indicate that current at 0.1 V increased slowly, reaching *ca.* 1.35 mA cm^{-2} at the end of 3 h test. When polarized at 0.7 V an initial current drop was seen, followed by a current recovery reaching a relatively stable current of *ca.* 5.20 mA cm^{-2} by the end of the 3 h test.

Comparing the steels with the carbon composite, the currents for 316 L and 317 L in the PAFC anode environment (2.85 mA cm^{-2} and 2.35 mA cm^{-2}, respectively) were higher than those of the carbon composite (1.35 mA cm^{-2}) under the same conditions, while the current for 904 L (1.43 mA cm^{-2}) was much closer to that of the carbon composite. In the PAFC cathode environment, the currents of 316 L (5.8 mA cm^{-2}) and 317 L (5.0 mA cm^{-2}) steels are at the same level as the carbon composite (5.2 mA cm^{-2}), while 904 L showed a much lower current of 1.7 mA cm^{-2}. This indicates that 904 L may be applicable as PAFC bipolar plate material, while significant improvement in surface coating or surface modification is needed before 316 L and 317 L could be used for this application.

These high currents indicate significant dissolution rates, and while metal ions are known to contaminate PEMFC membranes, reducing their performance, the impact of these ions on the performance of the PAFC is unknown.

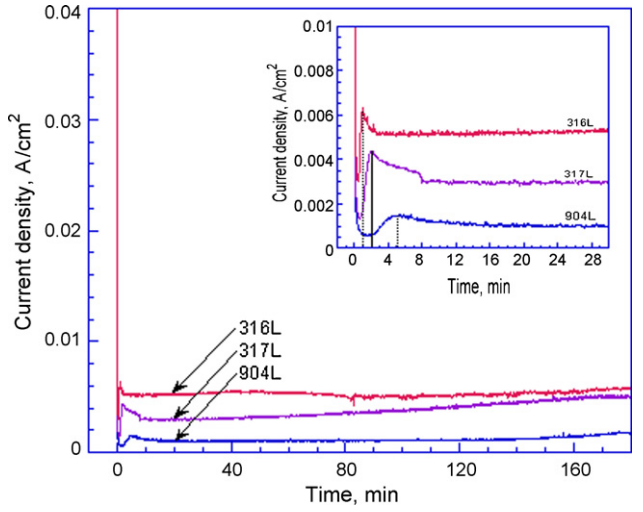

Fig. 3. Potentiostatic polarization of stainless steels at 0.7 V in H_3PO_4 at 170 °C purged with air. Inset shows the current decay during the first half hour of polarization.

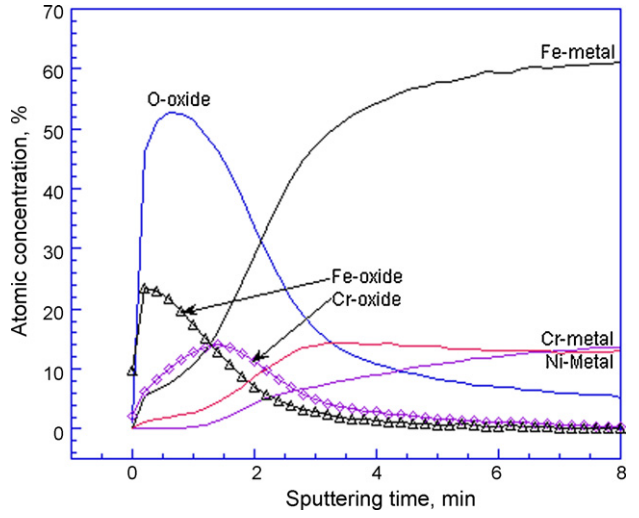

Fig. 5. XPS depth profile of fresh 316 L stainless steel.

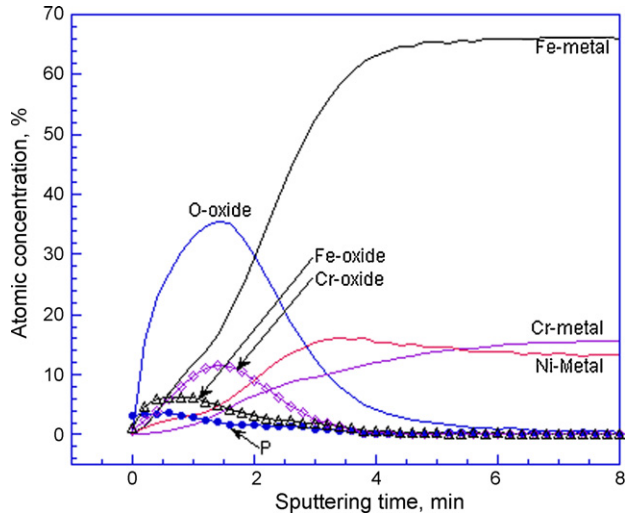

Fig. 6. XPS depth profile of 316 L steel after 3 h polarization at 0.1 V in 98% H_3PO_4 of 170 °C. The electrolyte was purged with hydrogen gas.

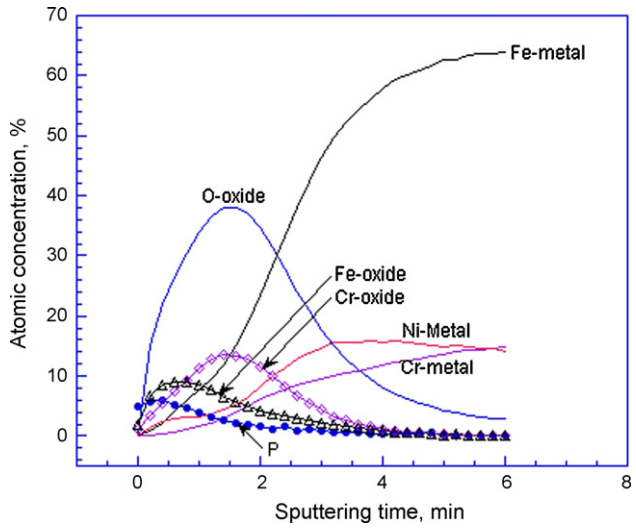

Fig. 7. XPS depth profile of 316 L steel after 3 h polarization at 0.7 V in 98% H_3PO_4 of 170 °C. The electrolyte was purged with air.

3.3. XPS depth profile

Except for the difference in bulk alloy content, the XPS depth profiles of these stainless steels are very similar to other fresh stainless steels [17–19]. The typical XPS depth profile of a fresh stainless steel is shown in Fig. 5, where 316 L steel is used. Again, the steel is covered with an air-formed oxide film composed of an Fe-oxide-rich outer layer and a Cr-oxide-rich inner layer. Ni and Mo (not shown) do not seem to participate in the surface oxides, though they have a significant influence on the stability of the surface film [20–22]. By using the half height of O-oxide as a measurement of the surface film thickness [23], the air-formed oxide film on 316 L requires approximately 2.4 min to sputter off. Adopting the sputtering rate of 14 Å min^{-1}, the surface oxide film is estimated to be 3.4 nm thick. This is similar to the air-formed film on 2205 [18], thinner than the surface oxide film on AISI446 [17], and thicker than the surface film on austenite stainless steel of 349 [19]. Fresh 317 L stainless steel has an air-formed film of *ca.* 2.7 nm thick, with a similar composition; and the air-formed film on fresh 904 L stainless steel is *ca.* 3.7 nm thick.

Fig. 6 shows the XPS depth profile of the 3 h polarized 316 L sample at 0.1 V with a hydrogen purge and Fig. 7 shows the XPS depth profile of 316 L after 3 h polarization at 0.7 V and air purged electrolyte. In both cases, the Fe-oxide is significantly depleted from the surface, leaving the Cr-oxide as the dominant surface oxide. This is similar to the passive film formation of the stainless steels in PEMFC environments [17–19]. Moreover in both figures, we see that phosphorus is incorporated into the outer part of the passive film. Clearly, the passive films formed on stainless steels in PAFC environments are different in chemical composition from those formed in the PEMFC environments. This process could plausibly occur concurrently with the dissolution of the Fe-oxide, though the mechanism at this time is far from clear. This is a specific phenomenon for the passive film formation on the stainless steels in PAFC environments. The passive film thickness on 316 L is estimated to be 3.8 nm in the PAFC anode environment and 4.1 nm in the PAFC cathode environment. Passive film formed on 317 L is 4.2 nm thick in the PAFC anode environment and 4.6 nm thick in the PAFC cathode environment. 904 L has a passive film thickness of 4.4 nm in both PAFC environments. These passive films are thicker than the passive films formed in PEMFC environments, where the thickness is normally less than 3 nm [17–19]. The high currents in PAFC environments (Figs. 2 and 3) are likely the major reason for these thicker passive films.

4. Conclusions

Austenite stainless steels 316 L, 317 L, and 904 L have been investigated in 98% H_3PO_4 at 170 °C. Dynamic polarization experiments revealed that the steels experienced passivation, regardless of the purged gases. When potentiostaticly polarized at 0.1 V (hydrogen) and 0.7 V (air) we observed high currents at the level of mA cm^{-2}. Comparing these to the results from the carbon composite under identical conditions, 904 L showed lower currents than those of the carbon composite, while 316 L and 317 L will require improvements in the PAFC anode environment to lower the current.

XPS depth profiles of the fresh steels indicated that the surface film consists of a Fe-oxide-rich outer layer and a Cr-oxide-rich inner layer. After being polarized in the PAFC environments, the Fe-oxide layer was selectively dissolved and Cr-oxide dominates the passive film. Phosphorus is incorporated into the passive film during the process in PAFC environments, thus the passive film formed is different in chemical composition than that formed in the PEM environments. After 3 h of polarization, the passive films on 316 L are 3.8 nm and 4.1 nm in the PAFC anode and cathode environments, respectively; passive films on 317 L are 4.2 nm and 4.6 nm in PAFC anode and cathode environments, respectively; while 904 L has a passive film of 4.4 nm in both PAFC environments.

Even for 904 L with the lowest currents in these simulated environments, the currents are significant (mA cm^{-2}) indicating that thin metal foils of these alloys are probably not suitable for PAFC applications.

Note, we did not measure the interfacial contact resistance (ICR) of the materials in the PAFC application, due to the high anodic currents. With improved corrosion resistance, ICR of the materials at related condition would be tested for the feasible application.

Acknowledgements

The authors thank Dr. Glenn Teeter for his help in XPS investigation. Dr. Greg Pacifico of PlugPower is acknowledged for providing the carbon composite samples. This work was supported by the Hydrogen, Fuel Cells and Infrastructure Technologies Program of the US Department of Energy.

References

[1] B.C.H. Steele, A. Heinzel, Nature 414 (2001) 345.
[2] 2007 DOE Hydrogen Program Review Presentations, US DOE Hydrogen, Fuel Cells & Infrastructure Technologies Program, Washington, DC, 15–18 May, 2007.
[3] S. Srinivasan, B.B. Davé, K.A. Murugesamoorthi, A. Parthasarathy, A.J. Appleby, in: L.J.M.J. Blomen, M.N. Mugerwa (Eds.), Fuel Cell Systems, Plenum Press, New York, USA, 1993, pp. 48–49.
[4] V. Mehta, J.S. Cooper, J. Power Sources 114 (2003) 32.
[5] A. Hermann, T. Chaudhuri, P. Spagnol, Int. J. Hydrogen Energy 30 (2005) 1297.
[6] A. Shanian, O. Savadogo, J. Power Sources 159 (2006) 1095.
[7] H. Tawfik, Y. Hung, D. Mahajan, J. Power Sources 163 (2007) 755.
[8] S.-J. Lee, J.-J. Lai, C.-H. Huang, J. Power Sources 145 (2005) 362.
[9] A. Kumar, R.G. Reddy, J. Power Sources 129 (2004) 62.
[10] R.C. Makkus, A.H.H. Janssen, F.A. de Bruijn, R.K.A.M. Mallant, J. Power Sources 86 (2000) 274.
[11] D.P. Davies, P.L. Adcock, M. Turpin, S.J. Rowen, J. Power Sources 86 (2000) 237.
[12] A.K. Iversen, Corros. Sci. 48 (2006) 1036.
[13] M.C. Li, C.L. Zeng, S.Z. Luo, J.N. Shen, H.C. Lin, C.N. Cao, Electrochim. Acta 48 (2003) 1735.
[14] D.J.L. Brett, N.P. Brandon, J. Fuel Cell Sci. Technol. 4 (2007) 29.
[15] R.F. Silva, A. Pozio, J. Fuel Cell Sci. Technol. 4 (2007) 116.
[16] H. Wang, M.A. Sweikart, J.A. Turner, J. Power Sources 115 (2003) 243.
[17] H. Wang, J.A. Turner, J. Power Sources 128 (2004) 193.
[18] H. Wang, G. Teeter, J.A. Turner, J. Electrochem. Soc. 152 (2005) B99.
[19] H. Wang, J. A. Turner, ECS Trans. 1 (6) (Proton Exchange Membrane Fuel Cells V, in Honor of Supramaniam Srinivasan, in: T. Fuller, C. Bok, C. Lamy (Eds.), 2006, pp. 263–272.
[20] C.R. Clayton, Y.C. Lu, J. Electrochem. Soc. 133 (1985) 2465.
[21] I. Olefjord, B. Bros, U. Jelvestam, J. Electrochem. Soc. 133 (1985) 2854.
[22] E. De Vito, P. Marcus, Surf. Interface Anal. 19 (1992) 403.
[23] M.Z. Yang, J.L. Luo, Q. Yang, L.J. Qiao, Z.Q. Qin, P.R. Norton, J. Electrochem. Soc. 146 (1999) 2107.